Eur. Phys. J. D **24**, 303–306 (2003)
DOI: 10.1140/epjd/e2003-00114-9

THE EUROPEAN PHYSICAL JOURNAL D

Circles of DNA-linked gold nanoparticle strands

D. Lee, S. Lee, H. Kim, and D.-J. Jang[a]

School of Chemistry, Seoul National University, Seoul 151-742, Korea

Received 10 September 2002
Published online 3 July 2003 –

Abstract. DNA-connected strings of gold nanoparticles are arranged to form very uniformly annular arrays having various diameters of a few micrometers by adjusting evaporation conditions as well as the concentrations of gold nanoparticles and phosphorothioate-modified oligonucleotides. The circles are formed by the dry hole-opening mechanism rather than by the Marangoni effect. However, their sizes are very diverse and their circumferences are approaching to show single-particle thinness instead of close-packed particle cluster thickness owing to DNA-linked gold nanoparticle strands.

PACS. 81.16.-c Methods of nanofabrication and processing – 78.67.-n Optical properties of low-dimensional, mesoscopic, and nanoscale materials and structures – 81.07.-b Nanoscale materials and structures: fabrication and characterization

1 Introduction

There has been much theoretical and experimental interest in nanostructured materials of semiconductors, metals, and metal oxides [1–10]. Attention is being focused on questions that pertain to the preparation and characterization of nanocrystal superlattices [4,10–15]. With respect to superlattice formation, most experimental work has been directed at extended two- or three-dimensional close-packed structures [2,3,8,9,16] and molecular recognition processes. Self-assembly of molecules into supramolecular structures are generally employed to construct nanometer-scaled arrays. In particular, DNA has the appropriate molecular-recognition and mechanical properties. The attractive feature of DNA as a particle linker is that one can synthetically program interparticle distances, particle periodicity, and particle compositions by choosing proper oligonucleotides [14,15,17–20].

Annularly arrayed structures of nanoparticles formed in evaporating drops have been reported extensively [1,4,13,21–24]. The self-assembly of submicrometer rings from dodecanthiol-capped silver nanoparticles in hexane has been explained in terms of dry hole-opening effects on the dewetting layer of a very thin film [21,22]. The array of 0.9-μm rings, composed of close-packed silver nanoparticles, has elucidated that the interactions of particle-particle and particle-substrate account for the accumulation of particles on the rim of an opening hole. On the other hand, the polydisperse ring formation of barium hexaferrite nanoparticles in hexane is attributed to originate from magnetic dipolar interactions [9]. By controlling solvent evaporation rates, one can also prepare rings and hexagonal arrays utilizing Marangoni instabilities [4,25]. It has been demonstrated later [21] that two different organizing mechanisms are engaged in the formation of hexagonal arrays and ring structures. The hexagonal arrays are due to the Marangoni effect in the earlier time of evaporation while the rings are due the dry hole-opening effect in the later time when the film height decreases to a certain critical value.

This paper presents our experimental report on the formation of ring structures, the circumferences of which are approaching to show single-particle thinness. The formation mechanism of DNA-linked gold nanoparticle circles and the contributional roles of complementary oligonucleotides are explained as well.

2 Experimental

Gold colloids were prepared by the citrate reduction of $HAuCl_4$ [18]. The prepared gold nanospheres are reasonably monodisperse in size and have an average diameter of 12.6 nm. The concentration of gold nanoparticles was determined by measuring the absorbance at 520 nm, where the extinction coefficient of the plasmon absorption was reported to be 2.4×10^8 M^{-1} cm^{-1} [18]. A 5'-phosphorothioate-modified 21-base oligonucleotide of 5'(phosphorothioate)-ATA-ACC-ATT-GTA-AAT-TAA-TTA-3' [oligonucleotide **A**] and its complementary oligonucleotide of 3'-TAT-TGG-TAA-CAT-TTA-ATT-AAT-5'(phosphorothioate) [oligonucleotide **B**] were employed to link gold nanoparticles. The colloidal solutions of

[a] e-mail: djjang@plaza.snu.ac.kr

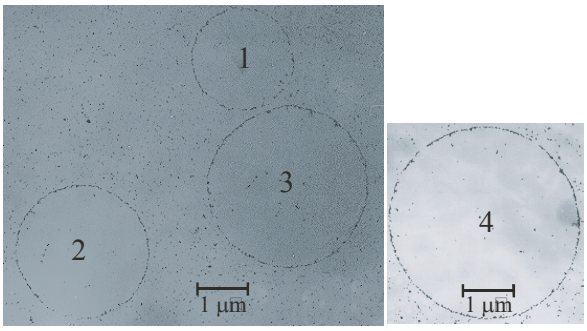

Fig. 1. TEM images for the typical ring-like structures of DNA-linked gold nanoparticles on carbon substrates.

Table 1. Diameters and ellipticities of gold nanoparticle circles in Figure 1.

circle number	1	2	3	4
d_{major} [a] (μm)	1.88	2.45	2.97	3.64
d_{minor} [b] (μm)	1.85	2.42	2.92	3.64
$d_{average}$ [c] (μm)	1.86	2.44	2.94	3.64
ε [d]	1.02	1.01	1.02	1.00

[a] The larger one of the horizontal and the vertical diameters.
[b] The shorter one of the horizontal and vertical diameters.
[c] The average of d_{major} and d_{minor}.
[d] The ratio of d_{major}/d_{minor}.

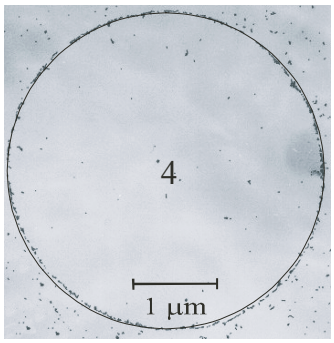

Fig. 2. The enlarged view of the ring structure 4 in Figure 1 and a fitted circle having a diameter of 3.64 nm (solid).

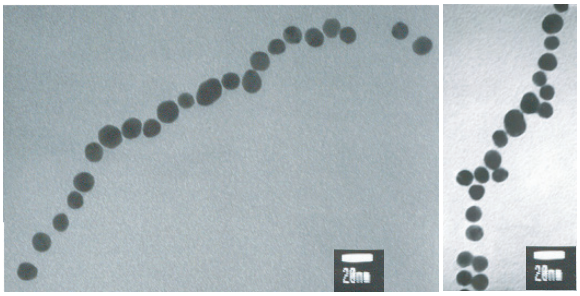

Fig. 3. Two closely viewed portions for the circumference of the ring structure 4 in Figure 1.

oligonucleotide **A**-modified (**A**-Np) and **B**-modified gold nanoparticles (**B**-Np) were prepared by derivatizing 25 mL of 9.29-nM gold nanoparticle solutions with 3.24 mL of 144-nM oligonucleotide **A** and **B** solutions (two oligonucleotides per nanoparticle in each solution), respectively, under vigorous stirring. The substituted phosphorothioate at the 5'-terminal makes the oligonucleotide adsorb to the gold nanoparticle surface. After being standed for a day, each solution was added with 3.24 mL of a solution containing 1-mM Tris buffer (pH 7.2), 5-mM EDTA, 5-M NaCl, and 0.1-μM PVP. Two equal volumes of **A**-Np and **B**-Np were mixed to prepare the colloidal solution of DNA-linked gold nanoparticle strands (**A**/**B**-Np). The concentration of each oligonucleotide in the final **A**/**B**-Np solution is the same as that of gold nanoparticles.

A drop of a colloidal solution was applied to an amorphously carbon-coated copper grid and allowed to evaporate at 50 °C in an oven for transmission electron micrographic (TEM) examination using a microscope (JEOL, JEM2000). Samples were contained in 1-cm quartz cells to take absorption spectra using a spectrophotometer (Sinco, UVS2040).

3 Results and discussion

The TEM images of Figure 1 show that annular structures of various sizes having very thin circumferences have formed during the evaporation of an **A**/**B**-Np solution. The diameters of the rings are a few micrometers and the rings are very uniformally circular (Tab. 1 and Fig. 2). The concentration of gold nanoparticles or DNA-linked gold nanoparticle strings is significantly smaller inside than outside the rings (Figs. 1 and 2). This suggests that the circles are formed by the dry hole-opening mechanism during the dewetting process of a colloidal solution [22,23]. At a certain critical value of the thickness of the colloidal solvent a hole opens up and grows to push the solvent and particles out toward the bulk film of the solution. Removed particles are accumulated on the hole rim and the advance of the growing hole is stopped when the radial force outward is no longer sufficient to overcome the frictional effects of the particles collected in the rim. So the resulting nanoparticle array takes the shape of a ring and particles become close-packed on the rim [21–23]. However, the observed diameters of our nanoparticle rings are very diverse ranging from 0.6 μm to 5 μm and nanoparticles are not close-packed on the rims. These indicate that the actual formation mechanism of our rings is quite different from the typical dry hole-opening mechanism. The ring sizes are expected to be the same at fixed values of the involved factors and the ring circumferences are close-packedly thick according to the typical hole-opening mechanism.

The closely viewed rims of nanoparticle rings presented in Figure 3 are approaching to show single-particle thinness and they are neither circular nor linear in the scale of a nanoparticle. These, together with the diverse sizes of nanoparticle rings, suggest that DNA hybridization plays an important role in the formation of the rings. To overcome the dragging force of the opening hole, a sufficient number of nanoparticles must accumulate along the rims.

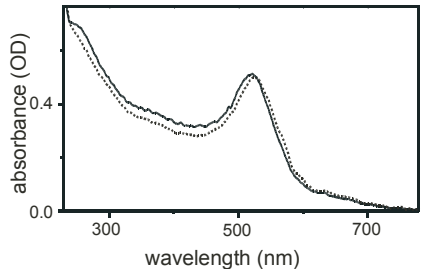

Fig. 4. Absorption spectra of **A**-NP (solid) and **A**/**B**-NP colloidal solutions (dotted).

We consider that the hydrogen bonding of hybridized DNA strands compensates for the particle-particle interaction to make DNA-linked nanoparticle strands constitute nanoparticle rings. In the conditions that the concentrations of each oligonucleotide in **A**/**B**-Np colloidal solutions are 2, 4, and 8 times as high as the concentration of gold nanoparticles, nanoparticles are agglomerated into larger clusters instead of forming any annular shapes. When the DNA concentration was one tenth of the nanoparticle concentration, gold nanoparticles were evenly dispersed in the carbon grid without forming circular or largely agglomerated structures. TEM specimens prepared at room temperature neither showed a regular annular pattern. So we suggest that the evaporation conditions and the relative and absolute concentrations of gold nanoparticles and oligonucleotides are crucial for the preparation of single-particle thin circles of gold nanoparticles.

The absorption spectra of Figure 4 show that the absorption of DNA at 260 nm decreases with the formation of doubly stranded helices while the surface plasmon absorption of gold nanoparticles at 523 nm shifts to the red by 4.4 nm with the formation of DNA-linked gold nanoparticle strands. The absorbance decrease of DNA around 260 nm signifies that the complementary oligonucleotides **A** and **B** form doubly helixed strands. The red shift of the plasmon absorption peak and the absorbance increase of the red region are consistent with reported observations [18]. However, our wavelength and absorbance changes are much smaller than the reported respective changes observed with gold nanoparticle aggregates having multiple DNA linkers per nanoparticle. It is reported [18] that the wavelength changes of nanoparticle aggregates with DNA linkers are related to the interparticle distance and that the absorbance changes are inversely dependent on the linker length. Considering the small changes of the gold plasmon absorption band with DNA connection and our low preparation temperatures of DNA connection and hybridization, we suggest that most gold nanoparticles are connected linearly in our experiments although the lengths of DNA-connected nanoparticle strands are very diverse. In other words, each of most nanoparticles is linked to two nanoparticles instead of multiple nanoparticles as seen in Figure 3.

What we have shown in the above can be summarized into several key issues. The circumferences of gold nanoparticle rings are mostly made of linear strands of DNA-connected gold nanoparticles. As a result, they are approaching to show single-particle thinness instead of close-packed particle cluster thickness. We believe that gold nanoparticle rings of single-particle thinness are prepared utilizing DNA connection for the first time. DNA hybridization compensates for the particle-particle interactions and it makes lesser nanoparticles overcome the dragging force of the opening hole. The formation of the rings is critically dependent on the relative and absolute concentrations of oligonucleotides and nanoparticles and the evaporation temperatures of TEM specimens. The red shift of the gold plasmon absorption at 523 nm and the absorption decrease of DNA at 260 nm suggest that oligonucleotide-modified gold nanoparticles are aggregated in the solution to form linear strings of DNA-connected gold nanoparticles. In particular, the small change of the gold plasmon absorption with aggregation and the single-particle thinness of gold nanorings indicate the formation of linear gold nanoparticle strings. The circular structures shown in TEM photographs designate that a dry hole-opening condition is the basic requirement in the ring formation of our experiments. However, our rings are very polydisperse in diameter and the circumferences are approaching to show single-particle thinness, indicating that the actual formation mechanism is quite different from the typical dry hole-opening mechanism. As the nanoparticles in a solution are aggregated in various lengths of linear strings, there is spatial inhomogeneity in the nanoparticle concentration of an evaporating drop on a copper grid. So the spatially different surface coverages result in various sizes of nanorings in the dewetting process. To clarify the roles of connecting oligonucleotides and the optimum conditions of evaporation for the formation of single-particle thin gold annular structures, more thorough inspection should be addressed.

The Seoul National University Development Fund (01-3-1) has supported this work. We also acknowledge the Center for Molecular Catalysis and the Brain Korea 21 Program.

References

1. S.L. Tripp, S.V. Pusztay, A.E. Ribbe, A. Wei, J. Am. Chem. Soc. **124**, 7914 (2002)
2. S.-J. Park, T.A. Taton, C.A. Mirkin, Science **295**, 1503 (2002)
3. J.M. Petroski, T.C. Green, M.A. El-Sayed, J. Phys. Chem. A **105**, 5542 (2001)
4. M. Maillard, L. Motte, M.-P. Pileni, Adv. Mater. **13**, 200 (2001)
5. C.S. Ah, S.D. Hong, D.-J. Jang, J. Phys. Chem. B **105**, 7871 (2001)
6. J.H. Chung, C.S. Ah, D.-J. Jang, J. Phys. Chem. B **105**, 4128 (2001)
7. C.S. Ah, H.S. Han, K. Kim, D.-J. Jang, J. Phys. Chem. B **104**, 8153 (2000)
8. C. Gutierrez-Wing, P. Santiago, J.A. Ascencio, A. Camacho, M. Jose-Yacaman, Appl. Phys. A **71**, 237 (2000)

9. K.V.P.M. Shafi, I. Felner, Y. Mastai, A. Gedanken, J. Phys. Chem. B **103**, 3358 (1999)
10. E. Braun, Y. Eichen, U. Sivan, G. Ben-Yoseph, Nature **391**, 775 (1998)
11. W. Fritzsche, Rev. Molec. Biotechnol. **82**, 37 (2001)
12. T.A. Taton, C. Lu, C.A. Mirkin, J. Am. Chem. Soc. **123**, 5164 (2001)
13. Y.W. Cao, R. Jin, C.A. Mirkin, J. Am. Chem. Soc. **123**, 7961 (2001)
14. S.-J. Park, A.A. Lazarides, C.A. Mirkin, P.W. Brazis, C.R. Kannewurf, R.L. Letsinger, Angew. Chem. Int. Ed. **39**, 3845 (2000)
15. L. He, M.D. Musick, S.R. Nicewarner, F.G. Salinas, S.J. Benkovic, M.J. Natan, C.D. Keating, J. Am. Chem. Soc. **122**, 9071 (2000)
16. S. Mann, W. Shenton, M. Li, S. Connolly, D. Fitzmaurice, Adv. Mater. **12**, 147 (2000)
17. R.C. Mucic, J.J. Storhoff, C.A. Mirkin, R.L. Letsinger, J. Am. Chem. Soc. **120**, 12674 (1998)
18. J.J. Storhoff, A.A. Lazarides, R.C. Mucic, C.A. Mirkin, R.L. Letsinger, G.C. Schatz, J. Am. Chem. Soc. **122**, 4640 (2000)
19. T. Torimoto, M. Yamashita, S. Kuwabata, T. Sakata, H. Mori, H. Yoneyama, J. Phys. Chem. B **103**, 8799 (1999)
20. A.P. Alivisatos, K.P. Johnsson, X. Peng, T.E. Wilson, C.J. Loweth, M.P. Bruchez Jr, P.G. Schultz, Nature **382**, 609 (1996)
21. C. Stowell, B.A. Korgel, Nano Lett. **1**, 595 (2001)
22. P.C. Ohara, W.M. Gelbart, Langmuir **14**, 3418 (1998)
23. P.C. Ohara, J.R. Heath, W.M. Gelbart, Angew. Chem. Int. Ed. Engl. **36**, 1077 (1997)
24. M. Elbaum, S.G. Lipson, Phys. Rev. Lett. **72**, 3562 (1994)
25. J.R.A. Pearson, J. Fluid Mech. **4**, 489 (1958)